

Synthesis and Evaluation of a ^{18}F -Labeled Diarylpyrazole Glycoconjugate for the Imaging of NTS1-Positive Tumors

Christopher Lang,[†] Simone Maschauer,[‡] Harald Hübner,[†] Peter Gmeiner,[†] and Olaf Prante^{*‡}

[†]Department of Chemistry and Pharmacy, Medicinal Chemistry, Emil Fischer Center, Friedrich Alexander University, Schuhstraße 19, 91052 Erlangen, Germany

[‡]Laboratory of Molecular Imaging and Radiochemistry, Department of Nuclear Medicine, Friedrich Alexander University, Schwabachanlage 6, 91054 Erlangen, Germany

S Supporting Information

ABSTRACT: Aiming to image NTS1 overexpressing tumors, the diarylpyrazole glycoconjugate **8**, derived from the potent NTS1 antagonist SR142948A, was synthesized taking advantage of the palladium-catalyzed aminocarbonylation reaction. The glycoconjugate **8** displayed excellent affinity and selectivity toward NTS1. Radiosynthesis proceeded straightforwardly, obtaining [^{18}F]**8** with excellent stability and highly beneficial biodistribution in vivo as demonstrated by PET imaging in HT29 tumor-bearing nude mice. Thus, the tracer [^{18}F]**8** represents a highly promising candidate for PET imaging of NTS1-positive tumors.

INTRODUCTION

Cancer is one of the leading causes of death worldwide. Among the different types, lung and bronchus, prostate, colorectum, pancreas, and breast carcinoma are especially responsible for the high mortality.¹ Therefore, the development of highly selective agents for therapy and also diagnostics is of particular importance. The G-protein-coupled neurotensin receptor 1 (NTS1)^{2,3} represents a very promising target for such agents, as it is overexpressed in a variety of tumors including the above-mentioned tumor types.^{4–6} In addition, NTS1 shows negligible expression in healthy tissues where these tumors arise from, making it a very specific molecular target for imaging and targeted cancer therapy.⁵ Until now, therapeutic approaches to treat NTS1-overexpressing tumors by addressing this receptor failed.⁷ However, as the abundance of NTS1 in tumors is very specific, various efforts in the development of both diagnostic radioligands to detect NTS1-positive tumors and agents for radiotherapy have been made.^{7–11} Positron emission tomography (PET) represents in principle a highly powerful diagnostic imaging tool, as it allows noninvasive in vivo imaging with excellent spatial resolution, high sensitivity, and precise quantification.¹² Until now, the development of NTS1 radiotracers that are applicable for PET was almost exclusively based on NT(8–13), which represents the active fragment of the peptidic endogenous NTS1 agonist neurotensin (NT, pE-L-Y-E-N-K-P-R-R-P-Y-I-L).^{7,13} However, peptidic radiotracers frequently reveal major disadvantages, primarily due to their instability in vivo because of degradation by endogenous peptidases,¹⁴ high kidney uptake in vivo that limits their applicability for radiotherapy,¹¹ and relatively low tumor retention that leads to decreased signal-to-noise ratios at late time points after tracer injection.

Recently, our group reported the synthesis of a metabolically stable ^{18}F -labeled NT(8–13) derivative by a click chemistry based ligation of the terminal alkyne bearing peptide with 2-deoxy-2- ^{18}F fluoroglucosylazide.¹⁰ The peptide-derived radiotracer **1** (Figure 1) showed excellent in vivo stability and was

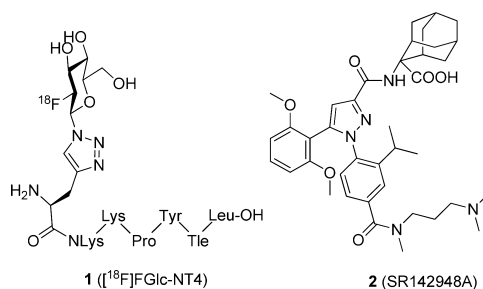


Figure 1. Structures of the peptidic NTS1 tracer **1** and the diarylpyrazole based NTS1 antagonist **2**.

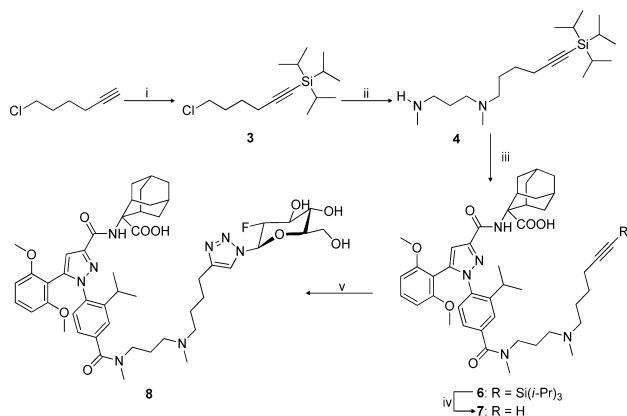
suitable for specific imaging of NTS1-positive HT29 tumors in nude mice by PET. However, in biodistribution studies the tracer revealed high kidney uptake and slow renal clearance. To improve this biodistribution pattern, we aimed at the development of a novel nonpeptidic radioligand based on the heterocyclic lead **2** (SR142948A, Figure 1), which has been described as a high affinity NTS1 antagonist displaying K_i in the low nanomolar range.¹⁵

In this work, we report the synthesis of a radiotracer with high affinity and excellent selectivity for NTS1 by taking advantage of our click chemistry based ligation of a terminal alkyne with 2-deoxy-2- ^{18}F fluoroglucosylazide. The alkyne bearing linker unit was introduced in one step, utilizing microwave assisted palladium-catalyzed aminocarbonylation reaction.^{16–18}

RESULTS AND DISCUSSION

To evaluate NTS1 binding affinity and selectivity over the subtype NTS2, the reference compound **8** bearing the stable fluorine isotope was synthesized according to Scheme 1. As preliminary experiments revealed that amines bearing terminal

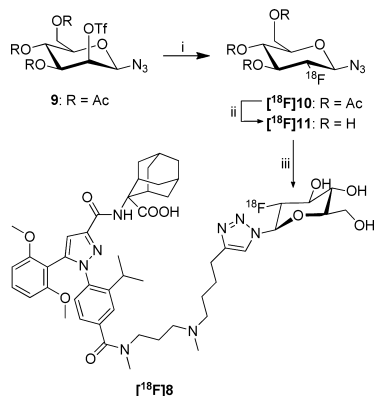
Received: September 25, 2013

Scheme 1^a

^aReagents and conditions: (i) (1) *n*-BuLi, THF, $-78\text{ }^{\circ}\text{C}$, 1 h, (2) TIPS-Cl, $-78\text{ }^{\circ}\text{C}$, 24 h (88%); (ii) MeNH(CH₂)₃NHMe, KI, K₂CO₃, MeCN, reflux, 69 h (89%); (iii) Mo(CO)₆, Herrmann's palladacycle, [(*t*-Bu)₃PH]BF₄, **5**, DBU, 1,4-dioxane, $140\text{ }^{\circ}\text{C}$, 30 min microwave (50%); (iv) TBAF, THF, rt, 3 h (83%); (v) 2-deoxy-2-fluoroglucosyl azide, CuSO₄·5 H₂O, sodium ascorbate, *t*-BuOH, H₂O, rt, 48 h (54%).

alkynes could not be converted to the corresponding amides by aminocarbonylation reaction, we aimed at the introduction of an alkyne protecting group. Therefore, commercially available 6-chloro-1-hexyne was deprotonated by *n*-BuLi and subsequently treated with TIPS-Cl to give the corresponding protected alkyne **3**.¹⁹ Treatment of **3** with *N,N'*-dimethylpropane-1,3-diamine afforded the protected diaminoalkyne **4**, which was converted to the corresponding amide **6**, employing microwave assisted palladium-catalyzed aminocarbonylation reaction of the previously reported aryl bromide **5**.²⁰ Removal of the protective group by TBAF led to the free alkyne **7** that served as precursor for the radiosynthesis of [¹⁸F]**8** (Scheme 2) or underwent CuAAC with 2-deoxy-2-fluoroglucosyl azide²¹ to give reference compound **8**.

Receptor binding data were determined in a competition binding assay using the radioligand [³H]neurotensin and stably transfected Chinese hamster ovary (CHO) cells expressing human NTS1 receptor. [³H]NT(8–13) was used for binding assays investigating human NTS2, which was transiently

Scheme 2^a

^aReagents and conditions: (i) [¹⁸F]F⁻, Kryptofix 2.2.2, K₂CO₃, KH₂PO₄, MeCN, $85\text{ }^{\circ}\text{C}$, 2 min (74% RCY); (ii) NaOH, $60\text{ }^{\circ}\text{C}$, 5 min (quant. RCY); (iii) HCl, **7**, sodium ascorbate, CuSO₄·5 H₂O, THF, EtOH, $60\text{ }^{\circ}\text{C}$, 10 min (70% RCY).

transfected in human embryonic kidney (HEK 293) cells. As shown in Table 1, the glycoconjugate **8** showed high NTS1

Table 1. Receptor Binding Data of **8 in Comparison to the Reference Agents Neurotensin, NT(8–13) and SR142948A Employing Human NTS1 and NTS2^a**

compd	K _i ± SEM (nM)	
	K _i (nM) NTS1 ^b [³ H]neurotensin	K _i (nM) NTS2 ^c [³ H]NT(8–13)
neurotensin	0.51 ± 0.060 ^d	4.9 ± 0.32
NT(8–13)	0.29 ± 0.032	1.4 ± 0.11 ^d
SR142948A (2)	1.0 ± 0.13	74 ± 14
8	0.98 ± 0.46	69 ± 20

^aK_i ± SEM are the means of 3–10 individual experiments each done in triplicate. ^bMembranes from CHO cells stably expressing human NTS1. ^cHomogenates from HEK cells transiently expressing human NTS2. ^dK_d ± SEM are the mean of 13–20 individual saturation experiments each done in quadruplicate.

affinity (0.98 nM) and substantial selectivity over the subtype NTS2 (70-fold). When compared to the affinity data of lead structure **2** (SR142948A), the conjugated sugar moiety did not infer the binding properties for NTS1 and NTS2 at all.

Because the glycoconjugate **8** revealed excellent in vitro binding data, we proceeded with the radiosynthesis of [¹⁸F]-labeled **8** and evaluated the radioligand in vitro and in vivo using tumor-bearing nude mice with NTS1-positive HT29 tumors. As shown in Scheme 2, the radiosynthesis started with the triflate precursor **9**,²¹ which underwent a cryptate-mediated nucleophilic substitution with no-carrier-added [¹⁸F]fluoride.²¹ The acetyl protective groups of the corresponding glucose derivative [¹⁸F]**10** were subsequently hydrolyzed under basic conditions to give unprotected [¹⁸F]**11**, which was employed in the CuAAC with the building block **7** (200 nmol), affording the NTS1 radiotracer [¹⁸F]**8**. The radiosynthesis followed our recent protocol,¹⁰ but THF had to be used as a solvent for the click conjugation step to preserve an optimal radiochemical yield (RCY). The preparation proceeded in a total synthesis time of 70 min, and [¹⁸F]**8** was obtained in a RCY of 20 ± 3% (uncorrected for decay, *n* = 6) and a high specific activity of 35–74 GBq/μmol. The log *D*_{7.4} determination of [¹⁸F]**8** revealed a value of -0.24 ± 0.02 . Stability experiments in vitro (human serum) and in vivo displayed excellent stability of [¹⁸F]**8**, as no degradation products could be observed (Supporting Information). To demonstrate specific binding of [¹⁸F]**8** in tissue, in vitro autoradiography studies of rat brain slices were conducted (Figure 2). The brain slices were incubated with 10 MBq of [¹⁸F]**8** in the presence or absence of various competitors.

Specific binding of [¹⁸F]**8** in NTS1-positive brain areas was demonstrated by competitive blocking with an excess of NT(8–13) and **2** (SR142948A). The use of NT led only to a partial decrease of radioligand binding which could be ascribed to the presence of distinct agonist NT and antagonist binding domains on the rat NTS1,²² in accordance with what has been reported for various other neuropeptide receptors.²³ The specific binding of [¹⁸F]**8** was evident especially in brain areas known to have a high NTS1 expression. The regional brain distribution of [¹⁸F]**8** is mainly in accordance with that of iodine-125-labeled NT.²⁴ Furthermore, using the NTS2 selective NT(8–13) derived peptide H-Arg-Arg-Pro-Nhtyr-

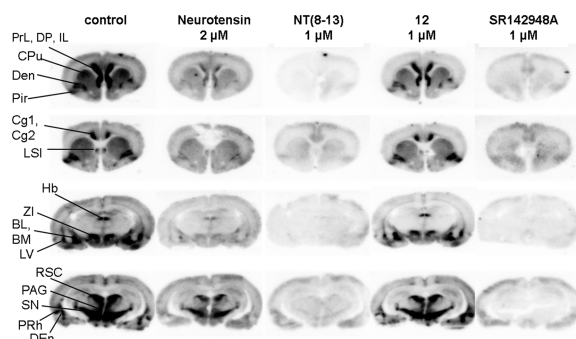


Figure 2. Autoradiography of rat brain slices after incubation with [^{18}F]9 in the absence (control) and presence of competitors. BL, basolateral amygdaloid nucleus; BM, basomedial amygdaloid nucleus; Cg1, Cg2, cingulate cortex area 1/2; CPU, caudate putamen; DEN, dorsal endopiriform nucleus; DP, dorsal peduncular cortex; Hb, Habenula; IL, infralimbic cortex; LSI, lateral septal nucleus; LV, lateral ventricle; PAG, periaqueductal gray; Pir, piriform cortex; PRh, perirhinal cortex; PrL, prelimbic cortex; RSC, retrosplenial cortex; SN, substantia nigra; ZI, zona incerta.

Ile-Leu-OH 25 (**12**) as competitor provided evidence for the high NTS1 selectivity of [^{18}F]8, as the binding of [^{18}F]8 in brain areas that are known to express NTS1 was fully unaffected in the presence of **12**, while binding of [^{18}F]8 in the marginally labeled NTS2-positive brain areas, such as cortex, was completely diminished. Furthermore, previously published results of autoradiography studies using a tritiated NTS1 ligand are in high agreement with the herein obtained results. 26

As the lead structure **2** has been described to cross the blood–brain barrier, 15 we were intrigued by the question of whether [^{18}F]8 could enter the brain in vivo. Therefore, we performed brain autoradiography studies with rats that were injected with [^{18}F]8, demonstrating that the radiotracer did not significantly cross the blood–brain barrier (data not shown).

Using HT29 tumor-bearing nude mice with a tumor diameter of 7–10 mm, we studied the suitability of [^{18}F]8 for imaging NTS1 expression in peripheral tumors. As shown in Figure 3A, the biodistribution of [^{18}F]8 in HT29 xenografted

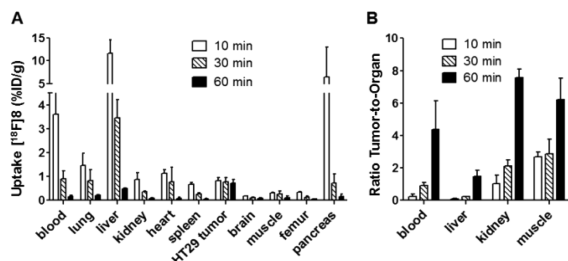


Figure 3. Biodistribution (A) and tumor-to-organ ratios (B) of [^{18}F]8 in nude mice bearing HT29 xenografts. Data are expressed as mean values \pm SD from two animals.

nude mice at 10, 30, and 60 min pi revealed fast blood clearance, fast clearance from the liver, and negligible uptake in the kidney, which is a highly beneficial in comparison to the high kidney uptake of most radiopeptides. In addition, [^{18}F]8 demonstrated high metabolic stability in vivo as determined by radio-HPLC of blood samples taken at 10 and 30 min postinjection ($>98\%$). Moreover, the uptake of [^{18}F]8 in HT29 tumors was $0.84 \pm 0.11\%$ ID/g early at 10 min pi and the tracer

demonstrated excellent tumor retention with an uptake of $0.74 \pm 0.14\%$ ID/g at 60 min pi (Figure 3A). Consequently, the tumor/blood ratios rapidly increased from 0.3 to 4.4 (10–60 min pi). A similar situation was observed for all other tumor/organ ratios as depicted in Figure 3B, suggesting a suitable signal-to-noise ratio for PET imaging. In comparison with the HT29 tumor uptake of already described NTS1-targeting radioligands, such as $^{99\text{m}}\text{Tc}$ -labeled peptides developed by Garcia-Garayoa et al. (6% ID/g), 8 ^{68}Ga - and ^{111}In -labeled NT derivatives by Alshoukr et al. (0.8–5% ID/g), 11 and our previously described ^{68}Ga -labeled peptoid (0.7% ID/g) 9 and ^{18}F -glycopeptoid **1** (1.2% ID/g), 10 the uptake value of [^{18}F]8 (0.74% ID/g) is within the low range. In this context, multimeric ligands consisting of multiple monomeric NTS1 ligands, as recently been studied, 27 could in principle lead to increased tumor uptake; however, a suitable multimeric NTS1 PET ligand has not yet been reported. Most importantly, [^{18}F]8 revealed an outstanding tumor/kidney ratio of 8 at 60 min pi (Figure 3B), which is highly favorable for PET imaging and provides the major advantage of the non-peptide [^{18}F]8 compared with most peptide ligands that suffer from high kidney uptake and low tumor/kidney ratios of 2 8,10 or even below 1. 11 When [^{18}F]8 was injected into HT29 xenografted nude mice for PET imaging studies, the tracer revealed displaceable and specific NTS1-dependent tumor uptake that was verified by co-injection of the selective NTS1 ligand SR142948A (3 mg/kg) (Figure 4). The comparison between

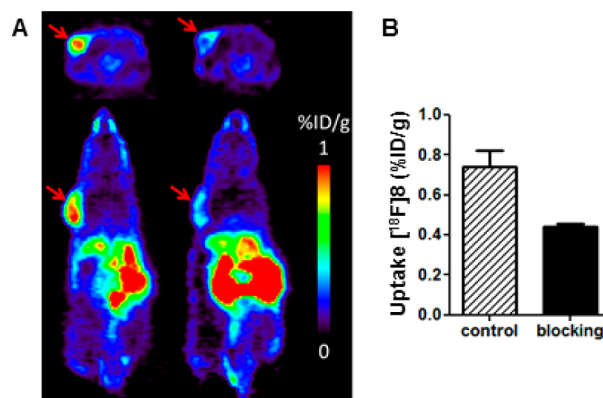


Figure 4. Small-animal PET imaging of [^{18}F]8. (A) Small-animal PET images (transaxial and coronal projections) of HT29 tumor-bearing nude mice at 45–65 min pi of [^{18}F]8 with (right) and without (left) co-injection of **2** (3 mg/kg). Red arrows indicate the tumor. (B) Tumor uptake (% ID/g) of [^{18}F]8 in HT29 xenografted nude mice 45–65 min pi determined by μPET . Data are expressed as mean values \pm standard error of the mean (SEM) from 4 animals.

control and co-injected animals demonstrated a significantly decreased tumor uptake in the coinjected animals by 40% (Figure 4B), thereby confirming specific visualization of NTS1 expression in HT29 tumors by [^{18}F]8 in vivo by PET.

In conclusion, we successfully developed the glycoconjugate [^{18}F]8 as the first non-peptide tracer for in vivo PET imaging of NTS1 expressing tumors, such as pancreatic, prostate, and mammary carcinoma. Because of its excellent clearance properties in vivo and high tumor retention, this tracer is a highly promising candidate for the translation into the clinic. Further preclinical studies of [^{18}F]8 and derivatives thereof using additional animal models are currently underway.

EXPERIMENTAL SECTION

General. The purity of the biologically evaluated **8** was $\geq 95\%$ as determined by HPLC. The radiochemical purity of [^{18}F]**8** prior to in vivo experiments was $>99\%$ (radio-HPLC). Full experimental protocols can be found in the Supporting Information.

Preparation of 8. To a solution of **7** (13.5 mg, 0.02 mmol) and 2-deoxy-2-fluoroglucosylazide (3.7 mg, 0.02 mmol) in *tert*-butanol/ H_2O (3 mL, 1:1) were added sodium ascorbate (0.36 mg, 1.8 μmol) and $\text{CuSO}_4 \cdot 5\text{H}_2\text{O}$ (0.23 mg, 0.9 μmol). After 48 h reaction at rt the reaction mixture was again treated with the same amount of sodium ascorbate and CuSO_4 and stirred for additional 24 h at rt. The mixture was filtered and purified by preparative HPLC to give **8** as a white lyophilisate (10 mg, 54% yield).

Radiosynthesis of [^{18}F]8**.** The mannosyl precursor **9** (7.5 mg, 16 μmol) in anhydrous acetonitrile (450 μL) was added to the dried $\text{K}^+/\text{Kryptofix 2.2.2}/^{18}\text{F}^-$ complex, and the solution was stirred for 2 min at 85 $^\circ\text{C}$. [^{18}F]**10** was isolated by semipreparative HPLC (Kromasil C8, 125 \times 8 mm, 4 mL/min, $\text{MeCN}/\text{H}_2\text{O}$ (0.1% TFA), gradient 30–70% in 30 min, $t_{\text{R}} = 9.5$ min) and trapped on a C18 cartridge (Lichrosorb, Merck, 100 mg). After elution with ethanol (0.8 mL) and evaporation of the solvent, a solution of NaOH (60 mM, 250 μL) was added. After 5 min at 60 $^\circ\text{C}$ (formation of [^{18}F]**11**), the pH was adjusted to 7–8 using 0.1 M HCl , followed by the addition of a solution of **7** (200 nmol in 400 μL of THF), CuSO_4 (0.4 M, 20 μL), and sodium ascorbate (1.2 M, 20 μL). After the mixture had been stirred for 10 min at 60 $^\circ\text{C}$, [^{18}F]**8** was isolated by semipreparative HPLC (see above; $t_{\text{R}} = 7$ min). The product fraction was diluted in water and passed through a RP-18 cartridge. The product was eluted with a solution of ethanol/0.9% NaCl (1:1, 1 mL). For in vitro and in vivo experiments, the solvent was evaporated in vacuo and [^{18}F]**8** was formulated with PBS (pH 7). The procedure yielded [^{18}F]**8** in a radiochemical yield of $20 \pm 3\%$ (uncorrected for decay, $n = 6$) and a radiochemical purity of $>99\%$ in a total synthesis time of 70 min with a specific activity of 35–70 $\text{GBq}/\mu\text{mol}$.

ASSOCIATED CONTENT

Supporting Information

Further experimental details, analytical data, ^1H NMR spectra, production of [^{18}F]fluoride, synthesis, analysis, and evaluation of [^{18}F]**8** (stability, $\log D_{7,4}$ in vivo, in vitro experiments), binding experiments. This material is available free of charge via the Internet at <http://pubs.acs.org>.

AUTHOR INFORMATION

Corresponding Author

*Phone: +49 9131 85-44440. Fax: +49 9131 85-34440. E-mail: olaf.prante@uk-erlangen.de.

Notes

The authors declare no competing financial interest.

ACKNOWLEDGMENTS

The authors thank Bianca Weigel and Manuel Geithoff for expert technical support. This work was supported by the Deutsche Forschungsgemeinschaft (DFG, Grant MA 4295/1-2).

ABBREVIATIONS USED

CuAAC, copper-catalyzed azide–alkyne cycloaddition; NT, neurotensin; NTS1, neurotensin receptor subtype 1; NTS2, neurotensin receptor subtype 2; Nhtyr, *N*-2-(4-hydroxyphenyl)ethylglycine; NLys, *N*-carboxymethyllysine; RCY, radiochemical yield; Tle, *tert*-leucine; TIPS, triisopropylsilyl

REFERENCES

- (1) Siegel, R.; Naishadham, D.; Jemal, A. Cancer statistics, 2013. *CA Cancer J. Clin.* **2013**, *63*, 11–30.
- (2) Vincent, J. P.; Mazella, J.; Kitabgi, P. Neurotensin and neurotensin receptors. *Trends Pharmacol. Sci.* **1999**, *20*, 302–309.
- (3) White, J. F.; Noinaj, N.; Shibata, Y.; Love, J.; Kloss, B.; Xu, F.; Gvozdenovic-Jeremic, J.; Shah, P.; Shiloach, J.; Tate, C. G.; Grishammer, R. Structure of the agonist-bound neurotensin receptor. *Nature* **2012**, *490*, 508–515.
- (4) Wu, Z.; Martinez-Fong, D.; Tredaniel, J.; Forgez, P. Neurotensin and its high affinity receptor 1 as a potential pharmacological target in cancer therapy. *Front. Endocrinol.* **2012**, *3*, 184.
- (5) Dupouy, S.; Mourra, N.; Doan, V. K.; Gompel, A.; Alifano, M.; Forgez, P. The potential use of the neurotensin high affinity receptor 1 as a biomarker for cancer progression and as a component of personalized medicine in selective cancers. *Biochimie* **2011**, *93*, 1369–1378.
- (6) Reubi, J. C.; Waser, B.; Friess, H.; Buchler, M.; Laissue, J. Neurotensin receptors: a new marker for human ductal pancreatic adenocarcinoma. *Gut* **1998**, *42*, 546–550.
- (7) Myers, R. M.; Shearman, J. W.; Kitching, M. O.; Ramos-Montoya, A.; Neal, D. E.; Ley, S. V. Cancer, chemistry, and the cell: molecules that interact with the neurotensin receptors. *ACS Chem. Biol.* **2009**, *4*, 503–525.
- (8) Garcia-Garayoa, E.; Blauenstein, P.; Blanc, A.; Maes, V.; Tourwé, D.; Schubiger, P. A. A stable neurotensin-based radiopharmaceutical for targeted imaging and therapy of neurotensin receptor-positive tumours. *Eur. J. Nucl. Med. Mol. Imaging* **2009**, *36*, 37–47.
- (9) Maschauer, S.; Einsiedel, J.; Hocke, C.; Hübner, H.; Kuwert, T.; Gmeiner, P.; Prante, O. Synthesis of a Ga-68-labeled peptoid–peptide hybrid for imaging of neurotensin receptor expression in vivo. *ACS Med. Chem. Lett.* **2010**, *1*, 224–228.
- (10) Maschauer, S.; Einsiedel, J.; Haubner, R.; Hocke, C.; Ocker, M.; Hübner, H.; Kuwert, T.; Gmeiner, P.; Prante, O. Labeling and glycosylation of peptides using click chemistry: a general approach to ^{18}F -glycopeptides as effective imaging probes for positron emission tomography. *Angew. Chem., Int. Ed.* **2010**, *49*, 976–979.
- (11) Alshoukr, F.; Prignon, A.; Brans, L.; Jallane, A.; Mendes, S.; Talbot, J. N.; Tourwé, D.; Barbet, J.; Gruaz-Guyon, A. Novel DOTA-neurotensin analogues for In-111 scintigraphy and Ga-68 PET imaging of neurotensin receptor-positive tumors. *Bioconjugate Chem.* **2011**, *22*, 1374–1385.
- (12) Li, Z. B.; Conti, P. S. Radiopharmaceutical chemistry for positron emission tomography. *Adv. Drug Delivery Rev.* **2010**, *62*, 1031–1051.
- (13) Granier, C.; Vanrietschoten, J.; Kitabgi, P.; Poustis, C.; Freychet, P. Synthesis and characterization of neurotensin analogs for structure activity relationship studies—Acetyl-neurotensin-(8-13) is the shortest analog with full binding and pharmacological activities. *Eur. J. Biochem.* **1982**, *124*, 117–124.
- (14) Garcia-Garayoa, E.; Allemann-Tannahill, L.; Blauenstein, P.; Willmann, M.; Carrel-Remy, N.; Tourwé, D.; Iterbeke, K.; Conrath, P.; Schubiger, P. A. In vitro and in vivo evaluation of new radiolabeled neurotensin(8-13) analogues with high affinity for NT1 receptors. *Nucl. Med. Biol.* **2001**, *28*, 75–84.
- (15) Gully, D.; Labeeuw, B.; Boigegein, R.; OuryDonat, F.; Bachy, A.; Poncelet, M.; Steinberg, R.; SuaudChagny, M. F.; Santucci, V.; Vita, N.; Pecceu, F.; Labbe-Jullie, C.; Kitabgi, P.; Soubrie, P.; LeFur, G.; Maffrand, J. P. Biochemical and pharmacological activities of SR 142948A, a new potent neurotensin receptor antagonist. *J. Pharmacol. Exp. Ther.* **1997**, *280*, 802–812.
- (16) Schoenberg, A.; Heck, R. F. Palladium-catalyzed amidation of aryl, heterocyclic, and vinylic halides. *J. Org. Chem.* **1974**, *39*, 3327–3331.
- (17) Appukkuttan, P.; Axelsson, L.; Van der Eycken, E.; Larhed, M. Microwave-assisted, $\text{Mo}(\text{CO})_6$ -mediated, palladium-catalyzed aminocarbonylation of aryl halides using allylamine: from exploration to scale-up. *Tetrahedron Lett.* **2008**, *49*, 5625–5628.

- (18) Roy, S.; Roy, S.; Gribble, G. W. Metal-catalyzed amidation. *Tetrahedron* **2012**, *68*, 9867–9923.
- (19) Englert, B. C.; Scholz, S.; Leech, P. J.; Srinivasarao, M.; Bunz, U. H. F. Templated ceramic microstructures by using the breath-figure method. *Chem.—Eur. J.* **2005**, *11*, 995–1000.
- (20) Gmeiner, P.; Lang, C. Efficient synthesis of heterocyclic neurotensin receptor ligands by microwave-assisted aminocarbonylation. *Synthesis* **2013**, *45*, 2474–2480.
- (21) Maschauer, S.; Prante, O. A series of 2-*O*-trifluoromethylsulfonyl-*D*-mannopyranosides as precursors for concomitant ¹⁸F-labeling and glycosylation by click chemistry. *Carbohydr. Res.* **2009**, *344*, 753–761.
- (22) Labbe-Julie, C.; Botto, J. M.; Mas, M. V.; Chabry, J.; Mazella, J.; Vincent, J. P.; Gully, D.; Maffrand, J. P.; Kitabgi, P. [³H]SR 48692, the first nonpeptide neurotensin antagonist radioligand characterization of binding-properties and evidence for distinct agonist and antagonist binding domains on the rat neurotensin receptor. *Mol. Pharmacol.* **1995**, *47*, 1050–1056.
- (23) Betancur, C.; Azzi, M.; Rostene, W. Nonpeptide antagonists of neuropeptide receptors: tools for research and therapy. *Trends Pharmacol. Sci.* **1997**, *18*, 372–386.
- (24) Moyses, E.; Rostene, W.; Vial, M.; Leonard, K.; Mazella, J.; Kitabgi, P.; Vincent, J. P.; Beaudet, A. Distribution of neurotensin binding-sites in rat-brain—a light microscopic autoradiographic study using monoiodo [¹²⁵I] Tyr³-neurotensin. *Neuroscience* **1987**, *22*, 525–536.
- (25) Einsiedel, J.; Held, C.; Hervet, M.; Plomer, M.; Tschammer, N.; Hübner, H.; Gmeiner, P. Discovery of highly potent and neurotensin receptor 2 selective neurotensin mimetics. *J. Med. Chem.* **2011**, *54*, 2915–2923.
- (26) Betancur, C.; Canton, M.; Burgos, A.; Labeeuw, B.; Gully, D.; Rostene, W.; Pelaprat, D. Characterization of binding sites of a new neurotensin receptor antagonist, [³H]SR 142948A, in the rat brain. *Eur. J. Pharmacol.* **1998**, *343*, 67–77.
- (27) Röhrich, A.; Bergmann, R.; Kretzschmann, A.; Noll, S.; Steinbach, J.; Pietzsch, J.; Stephan, H. A novel tetrabranched neurotensin(8-13) cyclam derivative: synthesis, ⁶⁴Cu-labeling and biological evaluation. *J. Inorg. Biochem.* **2011**, *105*, 821–832.